

Two helical conformations of polythiophene, polypyrrole, and their derivatives

C. X. Cui* and Miklos Kertesz

Department of Chemistry, Georgetown University, Washington, D.C. 20057

(Received 12 June 1989)

Two stable conformations, a planar or nearly planar rod and a coil, have been located on the potential-energy surfaces of several conducting polymers: polythiophene (PT), poly(3-methylthiophene) (PMeT), polypyrrole (PPy), and poly(3-methylpyrrole) (PMePy). The planar structure is slightly more stable for PT, PPy, and PMePy, while the coil configuration is preferred for PMeT. This finding could explain the existence of the coil conformation for poly(3-butylthiophene) in solution and for doped PMeT and PPy in the solid phase. We have identified a quinoid coil form of PT by our calculations, which strongly supports the presence of a coil conformation of doped PT derivatives. The band gap and total energy as functions of the conformation of PT indicate that the thermochromic behavior of PT derivatives results from the change in conformation with temperature. Similar behavior is expected for PPy derivatives. Vibrational analysis for helical and planar conformations of PT has been carried out, which identifies experimental possibilities in distinguishing among the rod versus coil conformations.

I. INTRODUCTION

Polythiophene (PT) and polypyrrole (PPy) are two of the most important heteroaromatic conducting polymers which have been synthesized up to now, and their geometrical and electronic structures are the subject of intensive experimental and theoretical research.¹ Conducting polymers with conjugated π electrons are usually assumed to be planar, although effects of nonplanarity have been sporadically mentioned in the literature.²

Most recent experimental evidence shows that poly(3-butylthiophene) has a coil or helical conformation in solution, and upon doping it becomes rodlike with a more rigid structure.^{3(a)} Further independent experimental observations support this conclusion. Photoelectron spectra of 2-2'-bithiophene and 3-3'-bithiophene derivatives can be explained on the basis of a twisted ground-state structure.^{3(b)} Studies of ultraviolet-visible (uv) absorption spectra of undoped polythiophene derivatives show a blue shift and thus loss of conjugation with the increase of the size of the substituents.⁴ For poly(3-methylthiophene) the maximum of absorption is at 480 nm (2.58 eV), which corresponds to a relatively large value for conjugated polymers.^{4(a)} Poly(3,4-dimethylthiophene) and poly(3,4-diethylthiophene) have the absorption maxima at 330 and 280 nm (3.76 and 4.43 eV),^{4(a),4(b)} indicating nonplanar structures of the polymers. Also the absorption maximum of polythiophene derivatives strongly depends on the method of preparation, and can vary from 2.58 to 5.98 eV.^{4(c),1} On the other hand, it is assumed that doped poly(3-methylthiophene) (PMeT) is in a coil conformation from an x-ray diffraction study of poorly crystallized samples, where the percentage of crystallinity is low, less than 5%.⁵ The existence of such coil structure has been definitely confirmed recently for doped PPy by scanning tunneling microscopy (STM).⁶

As far as unsubstituted PT is concerned, it is in planar conformation in the solid state as demonstrated by recent

x-ray diffraction.⁷ This is in concordance with the crystal structure of 2-2'-bithiophene which has coplanar thiophene rings.⁸

Recent experiments indicate thermochromic behavior of PT derivatives,⁹ a behavior similar to that of the σ -polymer polysilane.¹⁰ The maximum of uv absorption shifts to larger wave numbers as the temperature is increased. In other words, the band gap becomes larger with the increase of temperature. For polysilane derivatives, such properties are attributed to the change in conformation with temperature.¹⁰ For PT derivatives, the reason for thermochromism is not clear, but it is certainly related to the change in conformation.⁹

In order to understand the new phenomena and novel structures related to PT and PPy derivatives, the geometrical and electronic structures of PT, PPy, and their derivatives will be studied by energy-band theory where a screw axis of symmetry has been taken into account. We show that in the undoped and doped state two conformations (a planar or close to planar structure which is called rod, and a coil structure) exist which are separated by a sizable barrier (about 3–6 kcal/mol). For the first time the energetics of helical conformations of PT, PPy, and their derivatives, including implications for the vibrational spectra, are discussed in this paper.

II. CALCULATION METHODS

At present, *ab initio* methods including fully geometric optimization are applicable for simple polymers like polyethylene, but in the case of polymers with medium-size unit cells (e.g., polythiophene) such calculations would still be formidable.¹¹ Therefore semiempirical approaches have to be used. It is well known that the modified neglect of diatomic overlap (MNDO) approach produces reasonable geometries of organic and inorganic molecules and polymers without using vast amounts of computer time.¹² Recent studies show that the predic-

tions of geometries of a number of organic and inorganic σ -bonded helical polymers are in overall agreement with experimental observations.¹³ In this work the MNDO crystal orbital approach¹² will be used to obtain the optimized bond lengths and bond angles of PT, PPy, and their derivatives. In the calculation, a screw axis of symmetry has been taken into account in order to simplify the calculation. More details about a screw axis of symmetry in polymeric band calculations can be found elsewhere.^{13,14} The EHT (extended Hückel theory)¹⁵ approach is used for the calculation of the band gap and the parameters are taken from Ref. 16.

It should be kept in mind that though the MNDO approach predicts rotational barriers moderately well, it is not highly accurate and usually underestimates the barrier by 1 kcal/mol on average.^{12(a)} Moreover, for some conjugated systems the MNDO approach fails in predicting the correct conformation. Therefore, before calculating the torsional potential curves of PT, PPy, and their derivatives, the reliability of the MNDO approach has to be examined. Table I lists the calculated torsional barriers of typical molecules by the MNDO approach, *ab initio* method at the STO-3G levels,¹⁷ EHT, and experiments.¹⁷ The EHT barriers have been obtained by the EHT total energies based on the MNDO fully optimized geometries at various rotational angles. It can be seen

TABLE I. Comparison of rotational barriers from different methods.

Molecules	Barriers (kcal/mol)			Expt. ^c
	MNDO	STO-3G ^a	EHT ^b	
CH ₃ -CH ₃	1.01	2.90	1.90	2.9
H ₂ CCH-CH ₃	0.17	1.40	1.05	1.85
CH ₃ -SiH ₃	0.38	1.30	0.84	1.7
CH ₃ -NH ₂	1.07	2.80	1.29	2.0
CH ₃ -PH ₂	0.64	1.90	1.61	2.0
CH ₃ -SH	0.52	1.50	0.65	1.3
CH ₃ -COH	0.18	1.37	0.48	1.16
BH ₃ -NH ₃	1.10	2.1	1.34	3.1
HS-SH (syn barr.)	4.88	6.1	7.33	6.8 ^d
(anti barr.)	1.92	2.9	0.84	6.8 ^d
CH ₂ -CH ₂	62.4	65.0	81.59	
NH ₂ -COH	3.57	24.7 ^e	25.86	21.3
C ₂ H ₃ -C ₂ H ₃ ^f	0.46	5.8	4.8	5.0
C ₆ H ₅ -OH	2.12	5.2	1.78	3.3
C ₆ H ₅ -NO	1.68	4.8	4.23	3.9
C ₆ H ₅ -CHO	— — — ^g	6.6	5.42	4.7
C ₆ H ₅ -NO ₂	— — — ^g	5.8	4.89	2.9
bithiophene	— — — ^g	4.5	4.68	5.0 ^h

^aTaken from Ref. 17.

^bThe barriers are calculated using the MNDO fully optimized geometries at various dihedral angles.

^cTaken from Ref. 17.

^dOnly a single barrier has been established.

^e4-31G

^fThe barriers around the single C—C bond of butadiene.

^gThe MNDO approach fails in predicting the planar structure as experimentally observed.

^hThis value is not in the gas phase, and it is determined by NMR from the oriented bithiophenes in liquid crystal solution [P. Bucci *et al.*, *J. Am. Chem. Soc.* **96**, 1305 (1974)].

that even though the MNDO approach uniformly underestimates the rotational barrier around σ bonds, the conformations of the corresponding molecules are correctly predicted, while it fails in predicting the planar conformation on some conjugated systems such as benzaldehyde and nitrobenzene. As a result, the MNDO approach could not be used for the calculation of conformations of conjugated systems. However, the MNDO approach produces reasonable bond lengths and bond angles. In other words, the MNDO approach can give us relatively accurate bond lengths and bond angles at various conformations except for the dihedral angles. In this way, if the MNDO optimized geometry is used to obtain the EHT total energy, it is possible to obtain a reasonable barrier and the correct conformation for the conjugated systems. Table I shows that such a combination results in not only reasonable barriers but also correct conformations. For the conjugated systems, the results are comparable to those from *ab initio* calculations at the STO-3G level. This combination of MNDO for bond distances and angles subsequently followed by EHT for rotational barriers and energy gaps, will be used throughout this paper. Of course, left-handed and right-handed helices have the same energy, and therefore need not be specified.

III. TORSIONAL POTENTIAL OF PT AND ITS DERIVATIVES

A. Dimers

It is worthwhile at first to perform calculations on bithiophene and its derivatives. The most stable form of bithiophene is calculated to be planar. The anti form [dihedral angle ($SC_\alpha C_\alpha S$) of 180°, Fig. 1(a)] is more stable than the syn one [the dihedral angle of zero, Fig. 1(b)] by 0.33 kcal/mol, which is not far from the value of 0.88 kcal/mol calculated by the *ab initio* method at the STO-3G* level where the *d* orbitals on the sulfur atom are included and its geometry is partially optimized.¹⁸ Recent experiments and theoretical calculations support the notion that the anti form is more stable, and indicate the

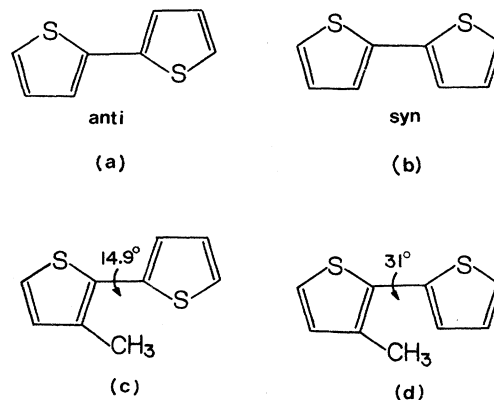


FIG. 1. Anti (a) and syn (b) conformations of bithiophene. Anti (c) and syn (d) conformations of bi-3-methylthiophene.

coexistence of anti and syn conformations.^{18,19}

The most stable conformation of bi-3-methylthiophene (BMeT) [Fig. 1(c)] is estimated to be slightly deviating from the anti planar structure by 14.9° (the dihedral angle is 165.1°). The second minimum [Fig. 1(d)] corresponds to the structure with a dihedral angle of 31.0° and is higher in energy than the first one by 0.69 kcal/mol. The two minima are separated by a barrier of 3.1 kcal/mol. These nonplanar structures can be attributed to the steric effects which come from repulsions between the methyl group and the sulfur atom.

B. Polythiophene

The importance of the coexistence of two stable conformations of bithiophene and its derivatives is that it leads to various stable forms of the corresponding polymers.

Figure 2 shows the torsional potential curve of PT calculated by the above-described combination of MNDO and EHT crystal orbital approaches. A screw axis of symmetry has been assumed and taken into account in the calculations.¹³ Two minima have been located on the energy surface. The first corresponds to the planar zig-zag (anti) conformation as shown in Fig. 3(a), in agreement with a recent x-ray diffraction investigation.⁷ The second is a helical conformation with a large helical radius (the largest distance between any atom of the repeat unit in a helical polymer and the screw axis). A completely planar syn conformation is impossible, since the molecule would coil back onto itself. If a conformation close to the planar syn structure could exist at all, it should form an ordered coil. Such a coil has a decreased delocalization energy and might have too high total ener-

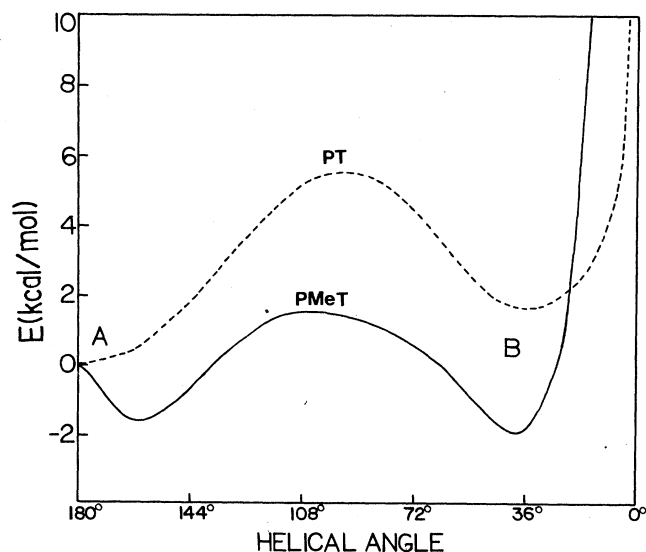


FIG. 2. Torsional potential curve of PT (dashed line) and PMeT (solid line) (the energy relative to anti conformation) calculated by EHT based on the MNDO fully optimized geometry. A and B correspond to the anti (rodlike) and syn (coil) conformations, respectively.

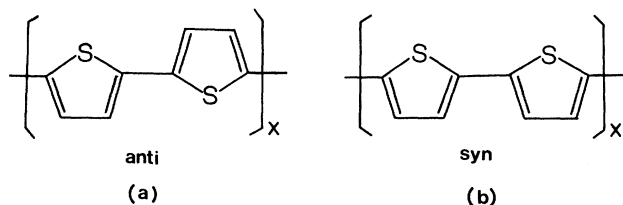


FIG. 3. Two alternative conformations of aromatic polythiophene: (a) anti and (b) syn.

gy to exist. The presence of the second minimum on the torsional potential curve (around $\theta=35^\circ$) indicates that such a conformation would actually be stable. As the dihedral angle is decreased to small values, the helical radius rapidly increases. The helical radii are 2.4, 2.3, 2.5, 3.3, 7.8, and 14.2 Å at helical angles of 180°, 144°, 108°, 72°, 36°, and 18°, respectively. However, for $\theta=0$ we can use the calculation of another conformation as shown in Fig. 3(b) which corresponds to infinite helical radius and has a very high energy due to angle strains which are necessary to make the chain linear. A helical angle of 35° is obtained at the minimum, and a planar projection of the coil structure at the minimum is shown in Fig. 4. Due to the overestimated long-range repulsion in the MNDO approach, the translational part of the screw operation is most likely to be exaggerated. By decreasing the translational part of the optimized geometry from

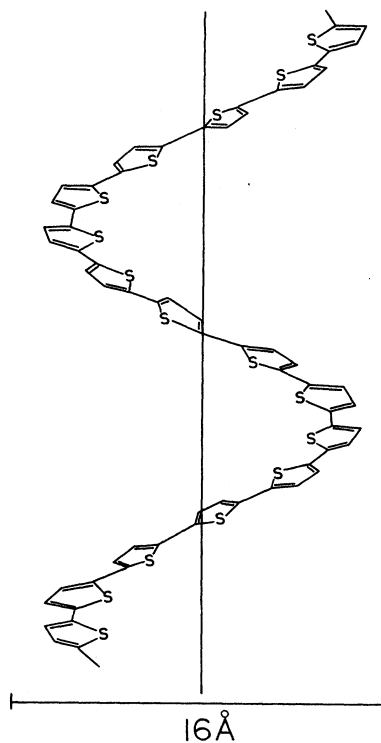


FIG. 4. The optimized geometry of PT with a coil conformation by the combination of the MNDO and EHT approaches (structure B in Fig. 2).

1.82 to 0.98 Å at a helical angle of 36°, the energy increases by a mere 0.23 kcal/mol. The planar structure is more stable than the coil by about 1.6 kcal/mol.

C. Polymethylthiophene

Figure 2 also shows the torsional potential curve of poly(3-methylthiophene). Due to the strong repulsion between sulfur and the adjacent methyl group, two nonplanar structures are predicted to be stable at helical angles of 159.9° and 34°, respectively. The latter helical angle is obtained in the same way as for PT and corresponds to a large helical radius of about 8 Å, and it has a coil confor-

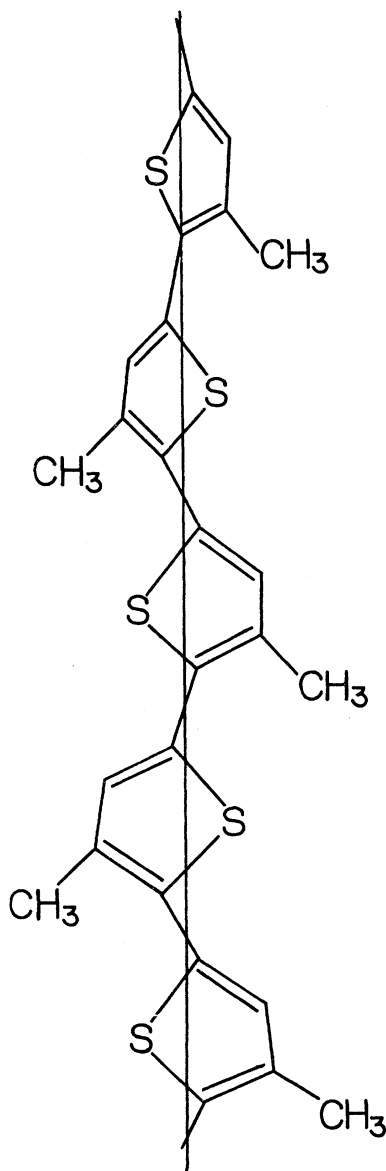


FIG. 5. The optimized geometry of PMeT with a rod conformation by the combination of the MNDO and EHT approaches (structure A in Fig. 2).

mation. The calculated coil structure of PMeT is very close to the one shown in Fig. 4 for PT. As we shall discuss later, this structure is related to the observed coil conformation of PMeT and PPy.⁵ The coil conformation for the undoped polymer with a large helical radius takes up more space than the rod structure and therefore is unlikely to occur in the solid phase if there are no other bulky side groups, and or dopants to support the coil. However, the coil structure could easily be stabilized in solution by solvent effects. This is in concordance with recent experimental observations.^{3(a)} For comparison, the rodlike structure is shown in Fig. 5. This rod structure is more stable than the anti coplanar one by 1.6 kcal/mol. Thus, taking crystal packing effects into account, the anti coplanar structure might be the most stable one in the solid state.^{7,20} It should be noted, however, that by further increasing the side groups, the energy difference between the perfect planar (anti) and rodlike structure (also anti) can be further increased. This seems to be a way to synthesize new conducting and at the same time optically active polymers.²¹

IV. BAND GAP AS A FUNCTION OF CONFORMATION

Thermochromism, as indicated in the Introduction, relates the energy gap to conformational changes.

Figure 6 shows the band gap as a function of the helical angle. These band gaps are calculated by the use of the MNDO optimized geometries of PT for several different fixed helical angles and are based on subsequent EHT band calculations using those MNDO optimized geometries. The band gap of 1.7 eV at a helical angle of 180° is near to the experimental value of 2.1 eV.²⁰ Themans *et al.* have shown by using their valence effective Hamiltonian (VEH) calculations that E_g will increase from 1.6 to 4.5 eV as the adjacent rings are rotated from $\alpha=0^\circ$ to 45° (maintaining an overall linear chain struc-

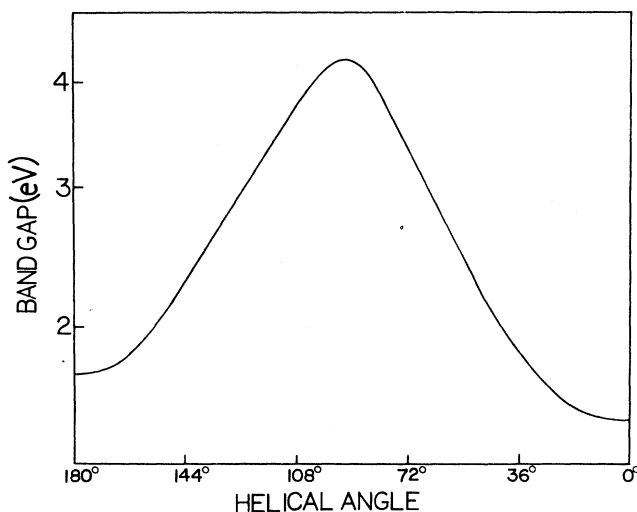


FIG. 6. EHT band gaps (eV) of PT as a function of the helical angle.

ture by rotating subsequent rings by $+\alpha$, $-\alpha$, $+\alpha$, $-\alpha$, etc.).^{9(b)}. In the present paper, we use standard EHT parameters for the calculation of the band gap.^{12(c)} Therefore the tendency of band-gap change upon the formation of the helix should be reliable, although absolute values are somewhat off, similarly to the VEH calculations.^{9(b)} While in earlier studies we have been able to fit the experimental E_g value of PT and its derivatives very well,^{12(c)} in the present paper we are only concerned with the qualitative effects caused by the transformations among the different helical conformations of conducting polymers. The maximum of the band gap occurs at the dihedral angle of about 90° , where no π interaction occurs between the rings. With the decrease of the dihedral angle from 90° , the band gap is decreasing again owing to the increase of the π interaction. The change of dihedral angle from 180° to 141° (the corresponding θ value is 144°) will increase the band gap by only 0.6 eV. Therefore a slight deviation from the coplanar (anti) structure of PT and its derivatives will lead to moderate increase in the band gap. Our conclusion concerning changes of the band gap as a function of the conformation is generally in agreement with Themans *et al.*,^{9(b)} a fact which should not be surprising in view of the great similarities of the two methods in question (EHT and VEH). However, Themans *et al.* did not predict the possibility of a small band gap for the coil conformation of PT. Let us note that we have obtained very similar relationships between E_g and the conformation for PMeT, PPy, and poly(3-methylpyrrole) (PMePy). Therefore we have not given the E_g versus θ curves for these materials here.

Let us return to the thermochromatic behavior of PT derivatives in the condensed phase and in solution. Thermochromism is most likely related to the fact that the planar or nearly planar structures have a smaller band gap than the higher-energy nonplanar structures. As the temperature is raised, thiophene rings may rotate away from those better overlapping and smaller-band-gap conformations in a statistical manner destroying translational symmetry in the case of the planar structure or helical

symmetry in the case of the ordered coil structure. Salaneck *et al.* have shown evidence for the reduction of the gap and conjugation as the temperature is increased.^{9(d)} Themans *et al.*^{9(b)} have offered an explanation if the low-energy structure is planar. According to our results, even if the low-energy form is a coil structure, such a reduction of E_g is expected because of the highly asymmetrical shape of the torsional potential curve around the minimum, and therefore, a rise in temperature leads to a shift of the average structure, corresponding to a larger average gap. Thermochromism for the coil structure is expected to be smaller than for the planar structure, since the E_g curve as a function of the dihedral angle does not have its minimum exactly at the same angle where the torsional potential does.

In both cases, thermochromism is expected to be accompanied by structure-dependent line shapes: The blue shift should occur together with a line broadening at higher temperatures. This is expected to be more pronounced if the minimum of the torsional potential is at an angle different from the minimum of E_g . The broadening effect described above is in agreement with the general experimental observations.⁹

V. POLYPYRROLE AND ITS DERIVATIVES

Potential curves similar to those of PT and PMeT have been obtained for PPy and PMePy as shown in Fig. 7. Each has two stable conformations, planar zigzag and coil. The planar zigzag structures of PPy and PMePy are more stable than the corresponding coil conformation by 2.2 and 3.9 kcal/mol, respectively. The steric effect arising from the presence of the methyl group is not very strong because the distance between the hydrogen atoms of the methyl group and the hydrogen atom on the N is larger than the sum of the van der Waals radii in the coplanar structure. A coil structure of doped PPy has been directly observed by STM.⁶ The similarity between the torsional potential curves in Figs. 4 and 6, and between the curves of the band gap as a function of conformation

TABLE II. Summary of geometrical parameters of undoped PT, PMeT, PPy, and PMePy at two stable conformations.

Polymer	Band gap ^a	$C_\alpha-C_\alpha^b$	$XC_\alpha C_\alpha X^c$	θ^d	R^e	Energy ^f
PT (rod)	1.70	1.446	180.0	180.0	2.4	0.0
PT (coil)	1.76	1.446	17.6	35.0	7.7	1.6
PMeT (rod)	1.88	1.450	158.2	159.9	3.7	0.4
PMeT (coil)	1.92	1.451	26.2	42.7	8.5	0.0
PPy (rod)	1.51	1.454	180.0	180.0	2.5	0.0
PPy (coil)	1.38	1.452	10.9	40.0	7.5	2.2
PMePy (rod)	1.55	1.457	180.0	180.0	3.8	0.0
PMePy (coil)	1.86	1.455	40.7	52.2	6.3	3.9

^aIn eV.

^bInterring bond distance in Å.

^cDihedral angle formed around interring bond in degree.

^dHelical angle in degree.

^eHelical radius in Å.

^fEnergy is given relative to the most stable conformation (in kcal/mol).

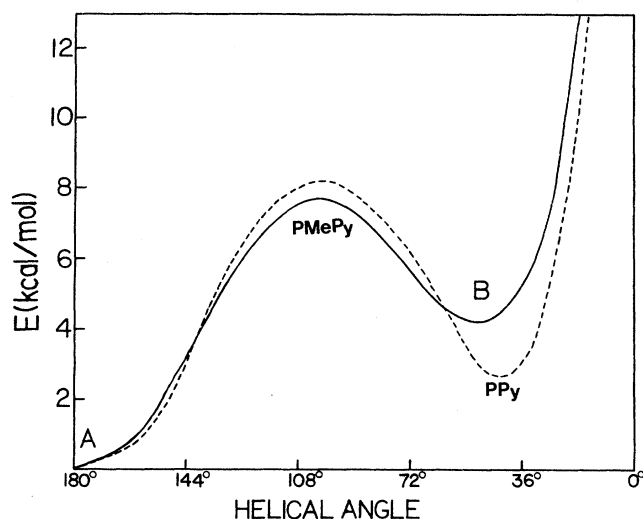


FIG. 7. Torsional potential curves of PPy and PMePY calculated by the EHT based on the MNDO fully optimized geometry. *A* and *B* correspond to the anti (rodlike) and syn (coil) conformations, respectively.

of polymer, indicate the possibility of thermochromism in PPy and its derivatives.

The important geometrical parameters and band gaps for PT, PMeT, PPy, and PMePy at the minima of energy surfaces are summarized in Table II.

VI. THE EFFECT OF DOPING ON GEOMETRY

In order to understand the effect of heavy doping on the conformation of PT derivatives, we have used charged clusters and their optimized geometries by the MNDO molecular-orbital approach, similarly to a study of the effect of doping on the geometry of polyacetylene.^{22(a)} Due to the limitations of the MNDO band theory, we have to use oligomer calculation, similar to earlier work by Brédas *et al.* for some conducting polymers.^{22(b)} In contrast to Brédas's approach, which included cations explicitly, we are interested here in the global effects of doping. We have omitted the cations from the calculations, since their locations are not known, and their effect is only of secondary importance with respect to our goal with these calculations, which is the interpretation of the observed coil to rod transition upon doping.

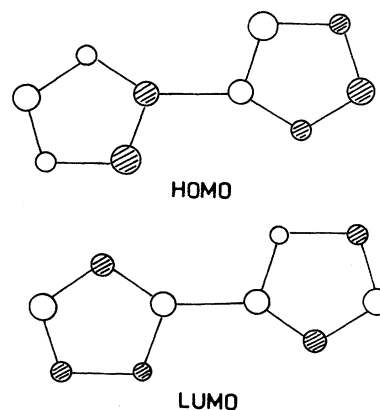


FIG. 8. The HOMO (highest occupied molecular orbital) and LUMO (lowest unoccupied molecular orbital) of 2-2'-methylbithiophene.

Table III lists the changes of the interring dihedral angles ($SC_{\alpha}C_{\alpha'}S$) of the neutral and charged bi-3-methylthiophene (charged by -2.0 and 2.0 electrons, which are the smallest amount of charge for closed shell calculations). It can be seen that upon charging positively or negatively, the optimized geometry of bi(3-methylethiophene) becomes planar.

Where does the driving force towards planarity for the charged oligomers come from? Figure 8 shows the HOMO (highest occupied molecular orbital) and LUMO (lowest unoccupied molecular orbital) of 2-2'-bi(3-methylthiophene), which corresponds to the crystal orbital in one unit cell at $k=0$ in the Brillouin zone.²³ The p_z orbitals of the HOMO on the atoms linking one ring to the next are antibonding. If one takes out an electron from bithiophene, the bonding between the two rings will be increased, and the planar geometry becomes favorable. The case of the LUMO is different. Addition of electrons to the LUMO will strengthen the bonding between the two rings, showing that the planar form is more stable again.

Another significant change in geometry of PT due to doping is that it goes from an aromatic form [Fig. 3(a)] to a quinoid form (Fig. 9). For example, the bond distances between thiophene rings of anti tetramer are 1.446, 1.447, and 1.446 Å while these values for the $2+$ charged tetramer are 1.381, 1.356, and 1.381 Å and for the $2-$ charged tetramer 1.383, 1.360, and 1.383 Å, respectively. Brédas

TABLE III. The change of dihedral angles^a of bi(3-methylthiophene) (BMeT) as a function of charge.

Molecule	BMeT ²⁺ anti	BMeT ²⁺ syn	BMeT ²⁻ anti	BMeT ²⁻ syn	BMeT anti	BMeT syn
Interring distance (Å)	1.360	1.361	1.369	1.370	1.451	1.451
Dihedral angle ^a	180.0	0.0	180.0	0.0	165.9	31.0

^aInterring dihedral angle ($SC_{\alpha}C_{\alpha'}S$) in degree, geometrical parameters optimized as described in text.

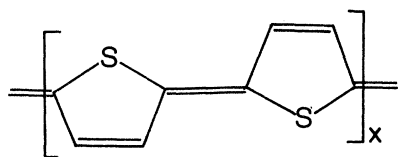
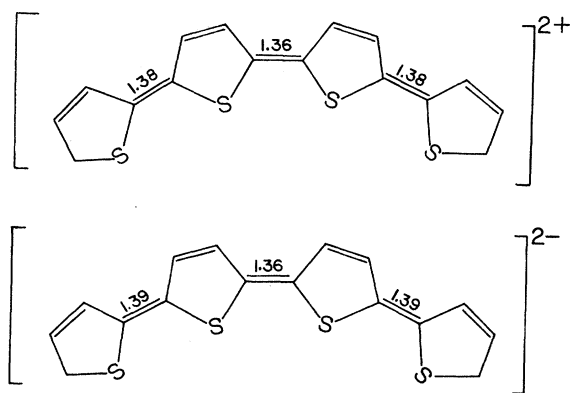
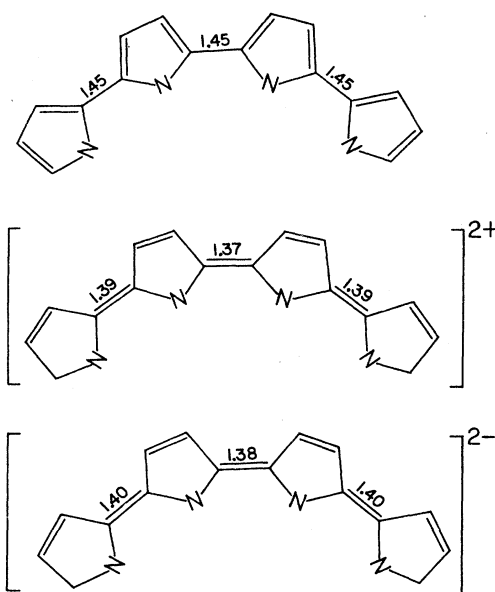


FIG. 9. The structure of the quinoid PT.

et al. have investigated the effect of doping by electron donors like Li and Na on the geometry of oligomers where the oligomer is assumed to have planar structure.^{22(b)} The doping by electron donors is equivalent to negatively charging the oligomer. The two approaches give very similar results as far as planar structures are concerned.

Let us turn to the discussion of structure of the highly doped (>20%) polymer chain (our discussion refers to high enough dopant concentration so that the bipolarons overlap and in fact cease to exist, and the structure of the whole system becomes quinoid). The doped anti structure is expected to become a planar quinoid chain. The doped syn structure, however, cannot be completely planar because the polymer chain has to bend back thereby forming a coil structure. This can be seen from Fig. 10, showing the MNDO optimized geometry of syn tetramers charged by $+2e$ and $-2e$. A completely similar result has been obtained for syn doped PPy as shown in Fig. 11.

In order to obtain further insight into the energetics of doped polythiophene, we have employed the following model. In contrast to studying the doped structure at a specific dopant concentration, we decided to study the energetics of the quinoid, but neutral (uncharged) form of PT. The results indicate structural trends only, since these do not correspond to a specific dopant concentration. Figure 12 indicates the existence of two structures on the potential-energy surface of quinoid PT similar to

FIG. 10. MNDO fully optimized geometries of tetrathiophene with $2+$ and $2-$ charges. (All-syn conformation.)FIG. 11. MNDO fully optimized geometries of neutral, $+2$ and -2 charged tetrapyrrole. (All-syn conformation.)

the aromatic form. In Fig. 12 the EHT energies of quinoid PT are shown as a function of the helical angle. For most of the values of the helical angle, the quinoid state does not even exist because the thiophene rings are rotated too much away from one another to maintain conjugation, and in these intermediate θ values (between $\approx 40^\circ$ and $\approx 145^\circ$) the calculations converge to the aromatic form of PT. There is a noticeable shift in the minimum towards a smaller θ value for the quinoid coil form. The minima are sharper than for the aromatic case. Therefore the *A* (anti, rod) conformation of the undoped substituted polythiophenes is expected to move towards a more planar conformation.

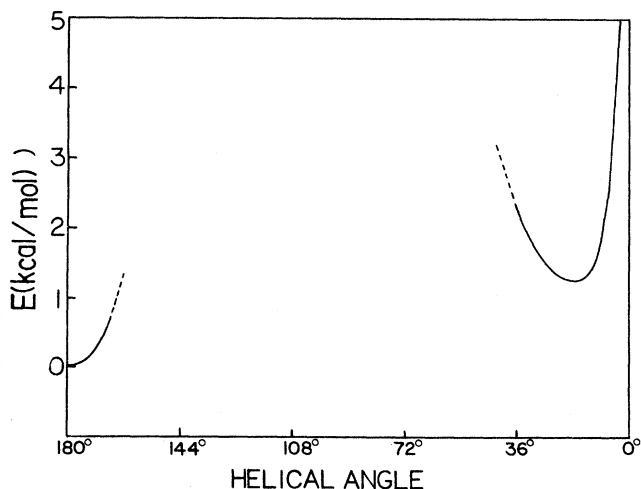
FIG. 12. The torsional potential curve of quinoid PT as a function of the helical angle. *A* and *B* correspond to anti (rod-like, planar) and syn (coil) conformations, respectively.

TABLE IV. Vibrational frequencies (cm^{-1}) of polythiophene with various conformations.

Helix ^a (TD) ^b	QPT ^c (TD)	APT ^d (TD)	Expt. (ir) ²⁷
797.5 (0.89)	895.2 (0.57)	818.4 (0.00)	827
914.4 (0.36)	906.1 (0.00)	898.0 (0.52)	860
920.2 (0.30)	986.8 (1.52)	923.0 (0.01)	922
990.0 (1.16)	988.6 (0.89)	984.4 (1.51)	1010
1008.8 (1.00)	1027.9 (0.86)	1003.5 (1.01)	1092
1023.6 (0.04)	1028.2 (0.00)	1013.9 (0.01)	
1026.8 (0.30)	1181.0 (0.01)	1022.4 (0.01)	
1149.9 (0.27)	1225.8 (0.28)	1177.4 (0.00)	
1189.7 (0.24)	1251.5 (0.18)	1212.2 (0.11)	1182
1283.9 (0.06)	1272.3 (0.01)	1292.5 (0.19)	1204
1286.9 (0.28)	1335.0 (0.02)	1310.8 (0.00)	1341
1326.6 (1.34)	1335.8 (0.80)	1348.7 (0.00)	1377
1369.0 (0.05)	1385.6 (0.02)	1390.6 (0.00)	
1423.4 (0.61)	1456.8 (0.95)	1412.0 (0.75)	1445
1427.2 (0.70)	1707.4 (0.01)	1449.6 (0.00)	1512
1597.8 (2.58)	1733.4 (0.38)	1593.6 (1.40)	1657
1682.0 (0.30)	1840.6 (0.38)	1670.8 (0.45)	1688
1798.1 (0.05)	1842.2 (0.03)	1734.4 (0.00)	
1817.4 (0.05)		1785.4 (0.00)	

^aHelical geometry of aromatic PT with helical angle of 90° .

^bTD, absolute values of transition dipole moment (in debye) are given in parentheses.

^cQuinoid PT, see Ref. 12(c).

^dAromatic PT, see Ref. 12(c).

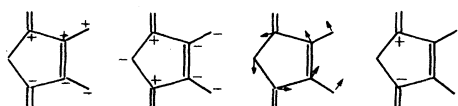
The above calculations establish the existence and nature of two forms, a rodlike and a coil form of both undoped (aromatic) and doped (quinoid) forms of substituted PT. Coil structures for (doped and undoped) substituted PT have been identified experimentally. The substitutions and relative energetics of these forms involve interactions with dopants and neighboring chains, which are beyond the scope of the present investigations.

VII. VIBRATIONAL SPECTRA OF PT

The ir and Raman spectra of several undoped PT derivatives have been reported.²⁴⁻²⁶ Although the assignments are not trivial, one may calculate the complete force field and perform a complete GF analysis^{27(a)} using the MNDO based force constants.^{27(b)} We have calculated vibrational frequencies of helical and planar PT's by the MNDO approach using numerical second derivatives in a Cartesian coordinate system maintaining translational or helical symmetry. We have not used any empirical scaling.²⁸ The calculated frequencies are shown together with the experimental ir data of poly(3-methylthiophene) in Table IV, in the wave number range of 800-1800 cm^{-1} . The transition dipole moments (TD) are also listed in Table IV, which can be used to determine which vibrational mode is ir active. If TD is not zero, the corresponding normal vibrational mode is ir active. These calculated frequencies correspond to the phonon wave vector of $\mathbf{k}=0$ in the Brillouin zone ("frozen phonon" approach).^{27(c)} For the helical conformation, a helical angle of 90° (dihedral angle of 104°) was chosen in order to obtain a large deviation from planarity. Each repeat unit contains two thiophene rings making the result with

those for the planar conformation easily comparable. The stretch vibrational frequency of C—H of the CH_3 group is about 3100 cm^{-1} , and it does not appear in the given frequency range. The deformational and rock vibrational frequencies of the CH_3 group are about 1550 and 950 cm^{-1} , respectively.^{26(a)}

A qualitative comparison of theoretical and experimental results is possible. First of all, it can be seen that there is no significant difference between the calculated vibrational spectra for the helical and planar models of PT. Naturally, the spectrum for the helical conformation is expected to be richer than the planar one because the former has more ir active vibrational modes due to the low symmetry. The experimental spectrum seems to be in slightly better agreement with those of the helical conformation of PT. However, further detailed experiments on unsubstituted PT are necessary to fully test the present theoretical result because the experimental spec-



COIL	268	403	475	713
PLANE	168	603	207	545

FIG. 13. Four vibrational modes which show the largest differences between the rod (anti) and the coil (syn) conformations of quinoid polythiophene.

tra are for PMeT. Further refinement of the theory will include force-constant scaling.²⁸

Table IV also shows the calculated vibrational frequencies for the quinoid form of PT (Fig. 9), which are very different from the experimental results, but in agreement with the generally accepted conclusion that the most stable ground state of PT is the aromatic form.²⁹ Extension for analogous systems, including polyisothianaphthene,²⁹ are in progress.

The calculated interring force constants $f(C_\alpha-C_\alpha)$ for the two forms of PT, aromatic and quinoid, are 6.97 and 9.84 mdyne/Å, respectively. Comparison of these values with the approximate force constants of 5.6 and 9.9 mdyne/Å for single and double C—C bonds^{26(a)} shows that there are double bonds between thiophene rings in the quinoid form of PT, while the bonds in the aromatic form of PT are essentially single bonds. Upon the formation of a helix, the force constant $f(C_\alpha-C_\alpha)$ for the aromatic form of PT does not change by more than 5%. This indicates that the π contribution to the C—C bond between thiophene rings is very small. Actually, earlier

calculation on bithiophene (aromatic) showed that the π contribution to the overlap population of this C—C bond is only 6%.^{17(c)}

Most of the calculated vibrational frequencies of the quinoid form of PT (planar rod and coil) are essentially identical except for some out-of-plane vibrations. The corresponding low-frequency modes together with their frequencies are shown in Fig. 13. For the rest of the calculated vibrational frequencies based on the two quinoid structures, the differences are less than 30 cm⁻¹. Some of these vibrational characteristics might be used to identify the various conformations of these conducting polymers.

ACKNOWLEDGMENTS

This work was supported by the National Science Foundation through a grant (DMR-8702148), and the Camille and Henry Dreyfus Foundation. Useful discussions with Dr. R. L. Elsenbaumer and L. Christensen are gratefully acknowledged.

*Permanent address: Institute of Theoretical Chemistry, Jilin University, Changchun, People's Republic of China.

¹(a) For a review see *Handbook of Conducting Polymers*, edited by T. A. Skotheim (Marcel Dekker, New York, 1986); (b) Proceedings of the International Conference on Science and Technology of Synthetic Metals [Synth. Met. C **28**, (1988)].

²(a) M. L. Elert and C. T. White, Phys. Rev. B **28**, 1013 (1983); (b) B. K. Roa, J. A. Darsey, and N. R. Kestner, *ibid.* **31**, 1178 (1985); (c) F. S. Bates and G. L. Baker, *Macromolecules* **16**, 1013 (1983).

³(a) J. P. Aime, F. Bargain, M. Schott, H. Eckhardt, G. G. Miller, and R. L. Elsenbaumer, Phys. Rev. Lett. **62**, 55 (1989); (b) P. Meunier, M. Caustale, C. Guimon, and G. Pfister-Guillouzo, J. Mol. Struct. **36**, 233 (1977).

⁴(a) G. Tourillon and F. Garnier, J. Electronal. Chem. **61**, 51 (1984); (b) J. W. Sease and L. Zechmeister, J. Am. Chem. Soc. **69**, 270 (1947); (c) E. K. Sichel, M. Knowles, M. Rubner, and J. Georges, Phys. Rev. B **25**, 5574 (1982).

⁵F. Garnier, G. Tourillon, J. Y. Barraud, and H. Dexpert, J. Mater. Sci. **29**, 2687 (1986).

⁶(a) R. Yang, K. M. Dalsin, D. F. Evans, L. Christensen, and W. A. Henderickson, J. Phys. Chem. **65**, 23 (1989); (b) W. R. Salaneck, R. Erlandsson, R. Prejza, I. Lundstrom, and O. Inganas, Synth. Met. **5**, 125 (1983).

⁷S. Bruchner and W. Porzio, Makromol. Chem. **89**, 961 (1988).

⁸G. J. Visser, G. J. Heeres, J. Wolters, and A. Vos, Acta Crystallogr. Sect. B **24**, 467 (1968).

⁹(a) S. D. D. V. Rughooputh, S. Hotta, A. J. Heeger, and F. Wudl, J. Polym. Sci. Polym. Phys. Ed. **25**, 1071 (1987); (b) B. Themans, W. R. Salaneck, and J. L. Brédas, Synth. Met. **28**, C359 (1989); (c) O. Inganas, G. Gustafsson, and W. R. Salaneck, *ibid.* **28**, C377 (1989); (d) W. R. Salaneck, O. Inganas, J. O. Nilsson, J. E. Osterholm, B. Themans, and J. L. Brédas, *ibid.* **28**, C451 (1989).

¹⁰R. West, J. Organomet. Chem. **300**, 327 (1986).

¹¹(a) A. Karpfen, J. Chem. Phys. **75**, 238 (1981); (b) H. Teramae, T. Yamabe, and A. Imamura, J. Chem. Phys. **81**, 3564 (1984).

¹²(a) M. J. S. Dewar and W. Thiel, J. Am. Chem. Soc. **99**, 4899

(1977); **99**, 4907 (1977); (b) J. J. P. Stewart, QCPE Bull. **5**, 61 (1985); J. J. P. Stewart, MOSOL Manual (USAF, Colorado Springs, 1984); (c) Y. S. Lee and M. Kertesz, J. Chem. Phys. **88**, 2609 (1988).

¹³C. X. Cui and M. Kertesz, J. Am. Chem. Soc. **111**, 4216 (1989).

¹⁴(a) A. Imamura and H. Fujita, J. Chem. Phys. **61**, 115 (1974); (b) I. I. Ukrainskii, Theor. Chim. Acta **38**, 139 (1975); (c) A. Blumen and C. Merkel, Phys. Status Solidi B **83**, 425 (1977).

¹⁵(a) R. Hoffmann, J. Chem. Phys. **39**, 1397 (1963); (b) M. H. Whangbo and R. Hoffmann, J. Am. Chem. Soc. **100**, 6093 (1978).

¹⁶J. K. Burdett, *Molecular Shapes* (Wiley, New York, 1980).

¹⁷(a) W. J. Hehre, L. Radom, P. v. S. Schleyer, and J. A. Pople, *Ab Initio Molecular Orbital Theory* (Wiley, New York, 1986); (b) P. W. Payne and L. C. Allen, in *Modern Theoretical Chemistry*, edited by H. F. Schaefer (Plenum, New York, 1977), Vol. 4; (c) J. L. Brédas, G. B. Street, B. Themans, and J. M. André, J. Chem. Phys. **83**, 1323 (1985).

¹⁸V. Barone, F. Leli, N. Russo, and M. Toscano, J. Chem. Soc., Perkin Trans. 2 **907** (1986), and references therein.

¹⁹P. Bucci, M. Longeri, C. A. Verracini, and L. Lunazzi, J. Am. Chem. Soc. **96**, 1305 (1974), and references therein.

²⁰T. C. Chung, J. H. Kaufman, A. J. Heeger, and F. Wudl, Phys. Rev. B **30**, 702 (1984).

²¹(a) R. L. Elsenbaumer, H. Eckhardt, Z. Iqbal, J. Toth, and R. H. Baughman, Mol. Cryst. Liq. Cryst. **118**, 111 (1986); (b) R. L. Elsenbaumer (private communication).

²²(a) M. Kertesz and F. Vonderviszt, Chem. Phys. Lett. **90**, 430 (1982); (b) J. L. Brédas, B. Themans, and J. M. André, Phys. Rev. B **26**, 6000 (1982).

²³(a) Y. Jiang, S. Alvarez, and R. Hoffmann, Inorg. Chem. **24**, 749 (1985); (b) C. X. Cui, Ph.D. thesis, Jilin University, 1987.

²⁴H. Neugebauer, G. Nauer, A. Neckel, G. Tourillon, F. Garnier, and P. Lang, J. Phys. Chem. **88**, 652 (1984).

²⁵G. Tourillon and F. Garnier, J. Phys. Chem. **87**, 2289 (1983).

²⁶H. Kuzmany *et al.* (unpublished).

²⁷(a) E. B. Wilson, Jr., J. C. Decius, and P. C. Cross, *Molecular*

- Vibrations* (McGraw-Hill, New York, 1955); (b) C. X. Cui, M. Kertesz, and J. J. P. Stewart (unpublished); (c) W. Weber, in *The Electronic Structure of Complex Systems*, edited by P. Phariseau and W. M. Temmerman (Plenum, New York, 1984).
- ²⁸P. Pulay, G. Fogarasi, G. Pongor, J. F. Boggs, and A. Vargha, J. Am. Chem. Soc. **105**, 7037 (1983).
- ²⁹(a) Y. S. Lee and M. Kertesz, Int. J. Quantum Chem. Symp. **21**, 163 (1987); (b) J. Kürti and P. R. Surján, (unpublished); (c) W. Wallnöfer, E. Faulques, H. Kuzmany, and K. Eichinger, Synth. Met. **28**, C533 (1989).